ELSEVIER

www.elsevier.nl/locate/jorganchem

Journal of Organometallic Chemistry 610 (2000) 58–70

Journal of Organometallic Chemistry

Structural and energetic aspects of hydrogen bonding and proton transfer to $ReH_2(CO)(NO)(PR_3)_2$ and $ReHCl(CO)(NO)(PMe_3)_2$ by IR and X-ray studies

Natalia V. Belkova [a], Elena S. Shubina [a], Evgenii I. Gutsul [a], Lina M. Epstein [a,*], Igor L. Eremenko [b], Sergei E. Nefedov [a,b]

[a] *A.N. Nesmeyanov Institute of Organoelement Compounds, Vavilov str. 28, V-334, Moscow 117813, Russia*
[b] *N.S. Kurnakov Institute of General and Inorganic Chemistry, Leninskii pr. 31, Moscow 177706, Russia*

Received 17 April 2000; received in revised form 27 June 2000

Abstract

The interaction of rhenium hydrides $ReHX(CO)(NO)(PR_3)_2$ **1** (X = H, R = Me (**a**), Et (**b**), *i*Pr (**c**); X = Cl, R = Me (**d**)) with a series of proton donors (indole, phenols, fluorinated alcohols, trifluoroacetic acid) was studied by variable temperature IR spectroscopy. The conditions governing the hydrogen bonding ReH···HX in solution and in the solid state (IR, X-ray) were elucidated. Spectroscopic and thermodynamic characteristics ($-\Delta H = 2.3–6.1$ kcal mol^{-1}) of these hydrogen bonded complexes were obtained. IR spectral evidence that hydrogen bonding with hydride atom precedes proton transfer and the dihydrogen complex formation was found. Hydrogen bonded complex of $ReH_2(CO)(NO)(PMe_3)_2$ with indole (**2a**–indole) and organyloxy-complex $ReH(OC_6H_4NO_2)(CO)(NO)(PMe_3)_2$ (**5a**) were characterized by single-crystal X-ray diffraction. A short NH···HRe (1.79(5) Å) distance was found in the **2a**–indole complex, where the indole molecule lies in the plane of the Re(NO)(CO) fragment (with dihedral angle between the planes 0.01°).

Keywords: Hydrides; Hydrogen bond; Protonation; IR spectroscopy; X-ray

1. Introduction

Since the discovery of unconventional hydrogen bonding with hydride ligand of transition metal hydrides (now referred to as 'dihydrogen bonding') several studies were performed either in solid state [1a–c] or in solution [1d,2]. The neutron diffraction and X-ray structures of intermolecular dihydrogen bonded complexes were obtained for the complex of $ReH_5(PPh_3)_3$ with indole and imidazole correspondingly [1b,c]. The IR and NMR spectral parameters and thermodynamic data for different systems involving intermolecular dihydrogen bonds were determined.

In the preliminary study of the interaction between $ReH_2(CO)(NO)(PR_3)_2$ (**1a–c**) and perfluoro-*tert*-butanol (PFTB) we demonstrated the competition between two sites of coordination: the oxygen atom of the NO-group and hydride ligand [2b]. Recently published results of NMR work [3] show the preference of hydrogen bonding to the hydride H_a ligand in the *trans* position to the NO-group in this system then dihydrogen bonding occurs. Here we present the detailed IR analysis of the effect of the ligand environment in rhenium hydrides $ReH_2(CO)(NO)(PR_3)_2$ (**1a–c**) and $ReHCl(CO)(NO)(PMe_3)_2$ (**1d**) and of proton donors nature on the site of hydrogen bonding. We compare the structures and energies of the dihydrogen bonded complexes in solution and in the solid state showing the strengthening of hydrogen bonded complexes of $ReH_2(CO)(NO)(PMe_3)_2$ upon going from solution to the solid state.

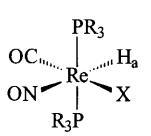

1
X = H_b, R = Me (**a**), Et (**b**), *i*Pr (**c**)
X = Cl, R = Me (**d**)

* Corresponding author. Tel.: +7-95-1356448; fax: +7-95-1355085.
E-mail address: epst@ineos.ac.ru (L.M. Epstein).

0022-328X/00/$ - see front matter
PII: S0022-328X(00)00416-2

The competition between the hydride and halogen ligands as well as the strong electronic influence of the latter on intramolecular dihydrogen bond strength have been found [1e] for iridium hydride complexes. Our present study of intermolecular hydrogen bonds in **1d** reveals the great preference of the Cl···HO bonds in the absence of any structural restrains. The participation of both classical (O···HO, Cl···HO) and unconventional (ReH···HO) hydrogen bonding in protonation of the hydrides **1** will be discussed.

2. Results and discussion

2.1. Hydrogen bonds of proton donors with rhenium hydrides

2.1.1. Structure in solution

The weak and medium strength proton donors (indole, phenol, 1,1,1,3,3,3-hexafluoro-2-propanol (HFIP), and perfluoro-*tert*-butanol (PFTB)) form hydrogen bonded complexes with rhenium hydrides. IR spectra of proton donors in the ν_{XH} range (at concentrations $C = 5 \times 10^{-3}$–1×10^{-2} M excluding self-association) in the presence of the hydrides **1a**–**c** ($c = 5 \times 10^{-2}$ M) reveal changes that are typical for hydrogen bond formation. The intensities of ν_{XH} bands of the free X–H-bond decrease and broad and intense low-frequency ν_{XH} bands of hydrogen bonded complexes appear. Spectral parameters of the $\nu_{XH\ bonded}$ bands such as the band shift $\Delta\nu = \nu_{XH\ free} - \nu_{XH\ bonded}$, half-height width ($\Delta\nu_{1/2}$), and integral intensity (A), increase with the proton donating ability growth: indole < phenol < HFIP < PFTB (Table 1). The isotopic ratio of the band frequencies $\nu_{OHbonded}/\nu_{ODbonded} = 1.35$ for the system HFIP·$ReH_2(CO)(NO)(PMe_3)_2$, is similar to that determined for classical medium strength hydrogen bonds with organic bases [4].

The compounds under investigation possess besides hydride atom several sites able to form hydrogen bonds: oxygen atoms of carbonyl and nitrosyl groups, chlorine and metal atom. Therefore it was necessary to establish the site of hydrogen bonding. This was done by the detailed variable temperature IR spectroscopy studies in the ranges of ν_L–ν_{CO}, ν_{NO}, ν_{ReH} and ν_{ReCl}– comparable to the earlier analyses of Ref. [2]. The general spectral criteria developed in those investigations are the following: (1) hydrogen bond formation with these ligands leads to the low frequency shift of the corresponding ν_L stretching bands; (2) the opposite high-frequency shift of ν_L indicates that this group does not act as a proton acceptor.

New high-frequency bands ν_{CO} ($\Delta\nu = 9$–12 cm^{-1}) appear in the ν_{CO} range of the IR spectra of **1** in the presence of equimolar amount or slight excess of the proton donors. The intensity of these bands increases on cooling and the reversibility of the temperature dependence indicates the reversibility of the process. The high-frequency position of the new ν_{CO} bands indicates that the carbonyl oxygen in the rhenium hydride complexes is not the site of hydrogen bonding [2a]. Furthermore the ν_{NO}, ν_{ReH} and ν_{ReCl} spectral ranges of these hydrides display individual changes under these conditions. The differences of spectral changes of the ν_L vibrations appeared to be connected with the competition between the nitrosyl oxygen (O_{NO}), the hydride and chlorine atoms as proton accepting sites.

Table 1
Spectral characteristics of ν_{XH} ($\Delta\nu$, $\Delta\nu_{1/2}$, A), enthalpies of hydrogen bond formation and basicity factors for hydrides **1**

	HX	ν_{XH}, cm^{-1} (A 10^{-4} M^{-1} cm^{-2})	$\Delta\nu$ cm^{-1}	$\Delta\nu_{1/2}$ cm^{-1}	$-\Delta H$ [a] ($-\Delta H$ [b]) kcal mol^{-1}	E_j [c]
1a	Indole	3400	100	70	2.3	0.79
	PhOH	3381 (5.8)	242	182	4.5 (4.4)	0.78 (0.77)
	HFIP	3334 (6.6)	277	248	5.0 (4.7)	0.82 (0.79)
	PFTB	3218 (8.7)	370	281	6.1 [d] (5.8)	0.80 (0.77)
1b	PhOH	3426	192	180	3.8	0.67
	HFIP	3404	207	200	4.0	0.68
	PFTB	3294	294	292	5.2	0.68
1c	PhOH	3460	163	135	3.3	0.58
	HFIP	3434	177	150	3.6	0.60
	PFTB	3347	243	250	4.5 [e]	0.60
1d	TFE	3429	199	146	3.9	0.77
	HFIP	3346	264	180	4.8	0.81
	PFTB	3233	356	240	6.0 [f]	0.79

[a] Enthalpies calculated from frequency shifts by Eq. (1).
[b] Enthalpies calculated from integral intensities by Eq. (2).
[c] $E_j = -\Delta H_{exp}/5.7P_i$.
[d] Values for $-\Delta H° = 5.8$ kcal mol^{-1}, $-\Delta S° = 6.3$ e.u. were obtained from temperature dependence of ln K.
[e] $-\Delta H° = 4.5$ kcal mol^{-1}, $-\Delta S° = 13.8$ e.u. from ln K versus $1/T$.
[f] $-\Delta H° = 5.7$ kcal mol^{-1}, $-\Delta S° = 9.6$ e.u. from ln K versus $1/T$.

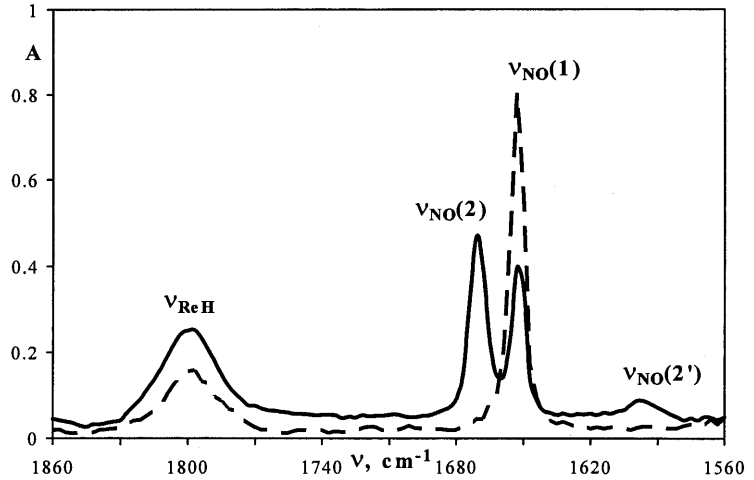

Fig. 1. IR spectra in the ν_{NO} and ν_{MH} range of the rhenium hydride **1a** (0.004 mol l^{-1}) (---) and of **1a** in the presence of PFTB (0.008 mol l^{-1}) (—) in hexane at 200 K.

The interaction between the proton donor and the hydride **1c** (X = H, R = *i*Pr) results in the exclusive formation of hydrogen bonded complex **2′c** with attachment at the O_{NO} atom: only broad low frequency ν_{NO} band characteristic for NO···HOR interaction appears [5a]. Its position and intensity depend somewhat on the proton donor strength. For example, $\Delta\nu_{NO}$ for hydrogen bonded complex **2′c** is -45 cm^{-1} with HFIP and -53 cm^{-1} with PFTB. The band intensity increases with the decrease of temperature. Notably, a broad ν_{ReH} band of low intensity ($A = 1.3 \times 10^{-4}$ M^{-1} cm^{-2}) does not change its position and intensity in the presence of alcohol and on cooling.

Quite different picture of interaction of the hydride **1a** (X = H, R = Me) with ROH proves that hydrogen bond forms to the hydride atom as a main site of coordination. A new high frequency band ν_{NO} ($\Delta\nu = +24$ cm^{-1}) corresponds to the hydrogen bonded complex **2a** of ReH···HOR type. The low frequency band similar to that of **2′c** has very low intensity demonstrating that the equilibrium content of the NO···HOR complex **2′a** is less than 6% (Fig. 1). The ν_{ReH} band broadens ($\Delta\nu_{1/2}$ increases from 30 in **1a** to 40 cm^{-1} in **2a**) and its integral intensity increases by factor of 1.5 (from 4.5×10^4 to 6.8×10^4 M^{-1} cm^{-2}, respectively). The explanation for this observation might be proposed taking into account the nature of the ν_{MH} bands in transition metal dihydrides. The analysis of IR and Raman spectra of hydride complexes of rhenium, molibdenum, tungsten etc. carried out in Ref. [6a] leads to the conclusion that only symmetric stretching vibrations bands appear in both spectra. In more recent work [6b], the ab initio calculations of MH_2 complexes (M = Ti, V) were performed and the results obtained were compared with experimental data. It was shown [6b] that symmetric (ν^s) and antisymmetric (ν^{as}) M–H stretching vibrations bands in IR spectra can appear near to each other and differ widely (for order) in intensity, the intensity of the ν^s_{MH} band being lower than that of the ν^{as}_{MH} band. In this connection we assumed the observed ν_{ReH} bands (around 1800 cm^{-1}) in the rhenium dihydride complexes **1a**–**c** to be an envelope of two bands of symmetric and antisymmetric vibrations ν_{ReH} while the changes of ν_{ReH} band in the presence of proton donors result from two counteracting effects. The formation of hydrogen bond to the one of hydride ligands should change the vibration modes: there should be a 'bonded' vibration with a low frequency shift whereas another band which attributed to vibrations of free Re–H group should undergo a slight shift in opposite direction. This situation is similar to that for stretching vibration bands of carbonyl groups [2a,7]. The observed increase of the integral intensity of this summary band is probably connected with the contribution of more intensive hydrogen bonded Re–H···H stretching vibrations. Although the IR study can not give more detailed structural information, the NMR results [3] provide evidences for the preferential binding to the H_a atom of **1a**, especially in the case of PFTB.

The more complicated situation is observed in the case of **1b** (R = Et). Here both types of hydrogen bonded complexes, ReH···HOR (**2b**) and NO···HOR (**2′b**), are in the equilibrium with the free **1b** molecules (Scheme 1).

New high frequency ν_{NO} band and low frequency shoulder on the ν_{ReH} band correspond to the complex **2b**. The intensities of these bands increase with the temperature decrease and these changes are similar to those observed earlier for the interaction between tungsten hydrides and proton donors [2a] indicating that the site of hydrogen bonding is the hydride atom. New low-frequency ν_{NO} band corresponds to the hydrogen bonded complex **2′b**. The positions of the ν_{NO} bands in the spectra of the hydrogen bonded complexes **2b** and

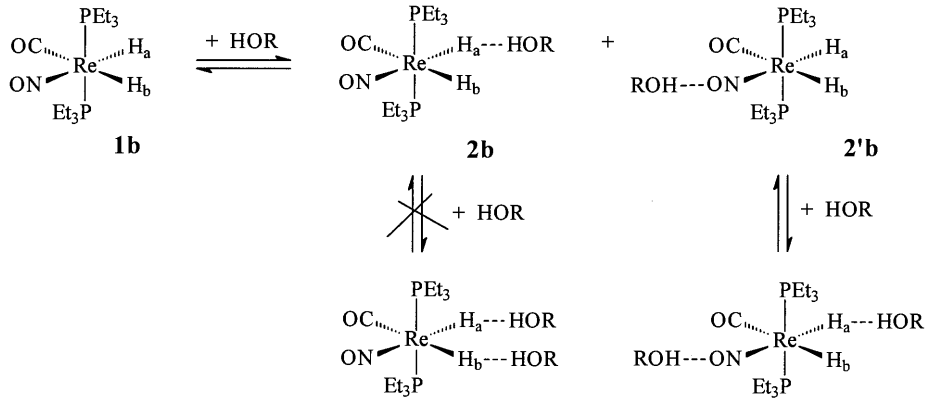

Scheme 1.

2′b depend considerably on the strength of proton donor: the $\Delta\nu$ values increase from HFIP to PFTB from $+13$ to $+17$ cm^{-1} in case of **2b** and from -48 to -58 cm^{-1} in the case of **2′b**. These IR findings are in good agreement with NMR observation [3] of co-existence of complexes **2b** and **2′b** with preferential Re–H_a···HOR binding.

Then comparing the hydrogen bonding pattern of the dihydride **1a** with that of the monohydride **1d** containing chlorine ligand we found the only one type of hydrogen bonding to **1d** which is ReCl···HOR. The IR spectra in the range of ν_{XH} of proton donors in the presence of the **1d** (in CH_2Cl_2 and hexane) showed the picture that is typical for hydrogen bond formation (Table 1). The variable temperature IR spectral study of the ν_L ranges revealed only high frequency shifts of the ν_{CO} ($\Delta\nu = +11$ cm^{-1}), ν_{NO} ($\Delta\nu = +16$ cm^{-1}) and ν_{ReH} ($\Delta\nu = +9$ cm^{-1}) stretching vibrations indicating that neither CO, NO nor ReH group acts as proton accepting site. The low-frequency shifts of the ν_{ReCl} band ($\nu_{ReCl} = 293$, $\Delta\nu = -13 \div -18$ cm^{-1}) were observed in the presence of proton donors (indole, HFIP, PFTB). The new ν_{ReCl}(bonded) band grows in intensity upon cooling or increase of proton donor concentration (Fig. 2). Recently similar effects were observed for OsCl···HOR^F hydrogen bonding in OsH(Cl)(CO)-(P^{t}BuMe$_2$)$_2$ system [8].

Summarizing at this point the results of the IR studies, we have seen that depending on the phosphine ligands proton donors can bind to the dihydride complexes **1a**–**c** via the hydride ligand preferably (**1a**), the hydride ligand and the O_{NO} atom (**1b**) or solely to the O_{NO} atom (**1c**). It is noteworthy that this order coincides with the increase of bulkiness of phosphine ligands (see next section for more detailed discussion). In the case of the monohydride **1d** electronic influence of chlorine ligand exerts a strong effect on hydrogen bonding site leading to inactivation of the hydride and O_{NO} sites and to formation of the ReCl···HOR adduct. The IR analysis advantageously allowed direct spectroscopic detection of the different hydrogen bonding adducts, because the equilibration rates for adduct formations are slow on the IR time scale.

2.2. Thermodynamics of hydrogen bonding in solution

Enthalpies of formation of hydrogen bonded adducts ($-\Delta H$) were determined from the correlation Eqs. (1) and (2) suggested by Iogansen [9] (Table 1):

$$-\Delta H = \frac{18\Delta\nu}{\Delta\nu + 720} \quad (1)$$

$$-\Delta H = 2.9\Delta A^{1/2} \quad (2)$$

The $-\Delta H$ and $-\Delta S°$ values for hydrogen bonded complexes of **2a** and **2′c** with PFTB in hexane were determined also from the temperature dependence of hydrogen bond formation constants (K). Experimental values of $K = [\mathbf{2}]/([\mathbf{1}]\cdot[\text{PFTB}])$ were determined by measuring the change of optical density of the $\nu_{CO\ free}$ and the $\nu_{NO\ free}$ bands over the temperature range of 200–270 K [10]. Temperature dependencies ln K versus $1/T$ for hydrogen bonded complexes of **1a** and **1c** with

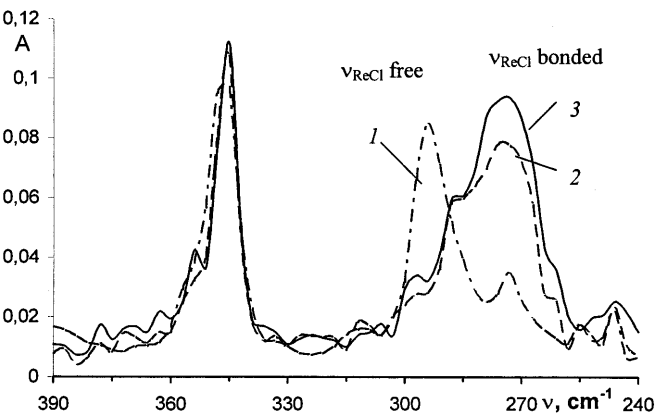

Fig. 2. IR spectra in the ν_{ReCl} range of the hydride **1d** (0.006 mol l^{-1}, 1) in the presence of 0.015 (2) and 0.030 (3) mol l^{-1} PFTB in hexane at 200 K.

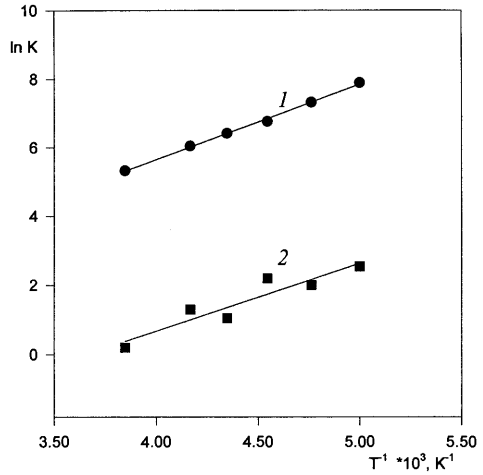

Fig. 3. The temperature dependence of ln K for hydrogen bonded complexes **2a** and **2′c** (HOR = PFTB).

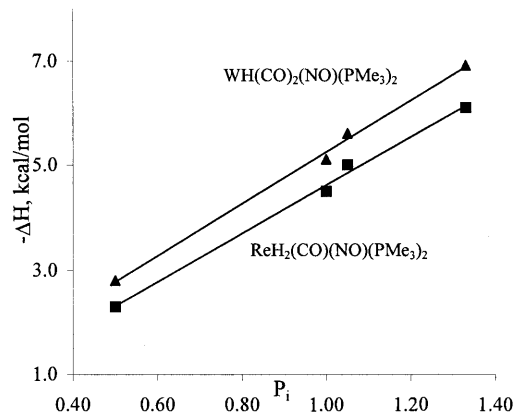

Fig. 4. Dependencies of the enthalpy values ($-\Delta$H, kcal mol^{-1}) of the hydrogen bonded complexes $MH^{\delta-}\cdots H^{\delta+}X$ (M = W, Re) on the acidity factors of proton donors (P_i [9b,11]).

PFTB are presented in Fig. 3. The obtained values are $-\Delta H° = 5.8 \pm 0.2$ kcal mol^{-1}, $-\Delta S° = 6.3 \pm 0.5$ e.u. for **2a** (X = H, R = Me), $-\Delta H° = 3.9 \pm 0.4$ kcal mol^{-1}, $-\Delta S° = 13.3 \pm 1.0$ e.u. for **2′c** (X = H, R = *i*Pr) and $-\Delta H° = 5.7 \pm 0.1$ kcal mol^{-1}, $-\Delta S° = 9.6 \pm 0.5$ e.u. for **2′d** (X = Cl, R = Me) with $R^2 = 0.997$–0.999. These enthalpy values are close to those determined from the empirical correlation Eqs. (1) and (2) (Table 1).

The existence of linear dependence between enthalpy values of **2a** and acidity factors (P_i) of proton donors similar to that found for WH···HX of $WH(CO)_2(NO)(PMe_3)_2$ [2a] (Fig. 4) confirms our earlier findings [2a,e] that the 'rule of factors' [11] proposed by Iogansen [9b] is applicable in the case of $XH^{\delta+}\cdots^{\delta-}HM$ type hydrogen bonds. Basicity factor (E_j) of the hydride atom in **1a** does not depend on proton donors as do the E_j values for organic bases [9] and metal atoms in organometallic compounds [2d,e]. It is smaller ($E_j = 0.80$) than those of tungsten hydrides $WH(CO)_2(NO)(PR_3)_2$ (R = Me, $E_j = 0.91$ and R = Et, $E_j = 0.87$), that is in agreement with the data [12] on ionic character of M–H bond (M = Re, W) in these hydride complexes. Analysis of the data obtained showed the dominant role of steric effect of PR_3 ligands in the competition of hydrogen bonding sites. The hydrogen bond OH···HRe does not appear in the case of $PR_3 = P^iPr_3$ with maximum steric hindrance (cone angle $\theta = 160°$ [13]) despite the maximal electron donating properties of this ligand which should increase the 'hydricity' of metal bound hydrogens. In this case nitrosyl group becomes the site of hydrogen bond formation. It is noteworthy that its proton accepting ability ($E_j = 0.60$), enthalpy ($-\Delta H° = 4.5$ kcal mol^{-1}), and formation constant (13 M^{-1} at 200 K) in the hydrogen bonded complex with PFTB are minimum and entropy value ($-\Delta S° = 13.8$ e.u.) is maximum. In the **1b** ($PR_3 = PEt_3$) hydride of modest basicity ($E_j = 0.69$) the decrease of steric hindrance of the phosphine ligand ($\theta = 132°$) results in the coexistence of two types of hydrogen bonded complexes **2b** and **2′b**. Further decrease of the cone angle ($\theta = 118°$) for $PR_3 = PMe_3$ is enough to gain in the competition by hydride ligand (despite the basicity of $PMe_3 < PEt_3$). Here the hydrogen bonded complex of OH···HRe type is dominant one with the maximum proton accepting ability ($E_j = 0.8$), the enthalpy ($-\Delta H° = 5.8$ kcal mol^{-1}) and the formation constant (1.6×10^3 M^{-1} at 200 K) of the hydrogen bonded complex with PFTB, and the minimum entropy change ($-\Delta S° = 6.8$ e.u.).

The results of ab initio calculations (density functional theory) of the model system $H_2Re(CO)(NO)(PH_3)_2 \cdot H_2O$ [2b] are in a good agreement with the experimental data. The calculated energy of hydrogen bonding with hydride atom (ReH···HO, 6.0–6.6 kcal mol^{-1}) in the absence of steric hindrance appeared to be more gaining in energy (for two times) than the interaction with NO- and CO-ligands. The energy of the DFT calculated ReH···H bond for CpRe(CO)(NO)H gave the same qualitative results [14], although the experiment performed for Cp*Re(CO)(NO)H ($E_j = 0.70$) [2c,d] showed the formation of both ReH···HO and NO···HO type complexes.

The $-\Delta H$ values for hydrogen bonded complexes of ReCl···HO type (**2d**) with HFIP and PFTB as well as the E_j values appear to be similar to those for ReH···H of **2a** though the entropy change is more significant. Such similarity is accidental but the absence of hydrogen bonding with hydride ligand in the presence of chlorine means that electronic effect of the latter leads to the decrease of hydride proton accepting ability in **1d**.

2.3. Structure of hydrogen bonded complexes in the solid state

We studied the interaction of **1a** with indole and *p*-nitrophenol in the solid state. The IR spectra of the hydrogen bonded complexes (films on CaF_2 and Nujol mulls) measured in the ranges of ν_{XH}, ν_{NO}, ν_{CO}, ν_{ReH} (Table 2) show that in the solid state intermolecular XH···HRe hydrogen bond not only retains but becomes stronger. The bands of the ν_{XH}(bonded) vibrations were observed at lower frequencies compare to hydrogen bonded complexes in solution (Tables 1 and 2). The shift values $\Delta\nu_{XH}$ for the hydrogen bonded complexes of **1a** with indole and *p*-nitrophenol are 195 and 250 cm^{-1}, respectively. In the range of stretching vibrations of the ligands the ν_{CO} and ν_{NO} bands of hydrogen bonded complexes are shifted to higher frequencies for 15–25 cm^{-1} in comparison with the initial hydride. The band ν_{ReH} is highly broadened in the spectra of films and the values of half-width ($\Delta\nu_{1/2}$) are 70 and 80 cm^{-1} for the complexes **2a**–indole and **2a**–*p*-nitrophenol, respectively. It is interesting that the spectra of crystalline hydrogen bonded complexes differ from that of films only in the range of ν_{ReH}. The two rather sharp bands ($\Delta\nu_{1/2}$ 34–45 cm^{-1}) one of them is shifted to low frequency range (Table 2, Fig. 5) are observed. The spectral characteristics indicate the stronger interaction XH···HRe in the solid state than that in solution. The formation enthalpy of the hydrogen bonded complex $H_2Re(CO)(NO)(PMe_3)_2$·indole (**2a**–indole) is almost twice higher in the solid state than that in hexane ($-\Delta H = 4.2$ and 2.3 kcal mol^{-1}, respectively).

Crystal suitable for X-ray diffraction studies was grown for the complex **2a**–indole. The complex is an adduct of **1a** and indole in accordance with the IR data (Fig. 6, Tables 3 and 4). The indole molecule is coplanar with the plane of the Re(NO)(CO) fragment (dihedral angle between these planes is 0.01°). The NO and CO groups are statistically disordered (Re–N(C) 1.866(9), 1.854(9) Å). Similar phenomena have been experienced in other M(NO)(CO) complexes as well [15]. The hydride atoms of **1a** and proton of the indole NH fragment were located and refined. The ReH_2 moiety contains two non-equivalent Re–H bonds (Re–H(1), 1.63(3); Re–H(2), 2.36(3) Å). At the first glance the Re–H(1) distance looks rather short but close values were observed earlier in phosphine car-

Table 2
IR data for $H_2Re(CO)(NO)(PMe_3)_2$ (**1a**) and its hydrogen bonded complexes with indole and *p*-$NO_2C_6H_4OH$ in the solid state (cm^{-1})

		ν_{XH} ($\Delta\nu$) [a]	ν_{CO}	ν_{ReH}	$\Delta\nu_{1/2}$(ReH)	ν_{NO}
1a			1942	1787	40	1628
1a+indole	Film	3277 (190)	1959	1786	70	1645
	Crystals [b]	3276 (191)	1959	1786	36	1645
				1748	45	
1a+*p*-$NO_2C_6H_4OH$	Film	3327 (260)	1964	1802	80	1647
	Crystals [b]	3327 (260)	1964	1794	34	1655
				1746	40	

[a] $\Delta\nu_{XH} = \nu_{XH\ free}$ (in CH_2Cl_2) $- \nu_{XH\cdots H}$ (crystal).
[b] In Nujol mull.

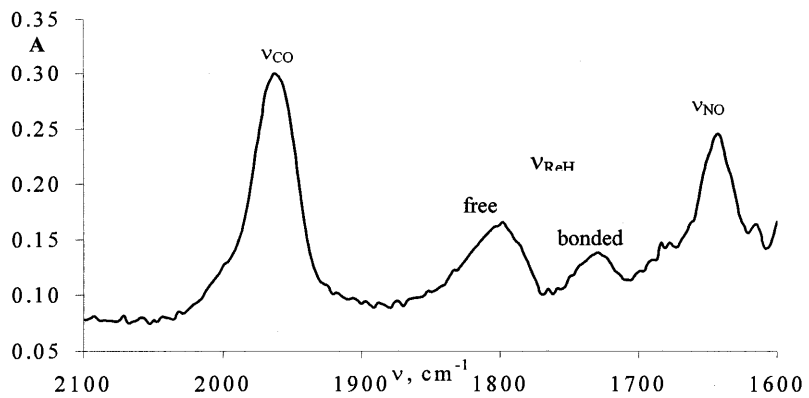

Fig. 5. IR spectra of the crystalline hydrogen bonded complex **2a**–indole.

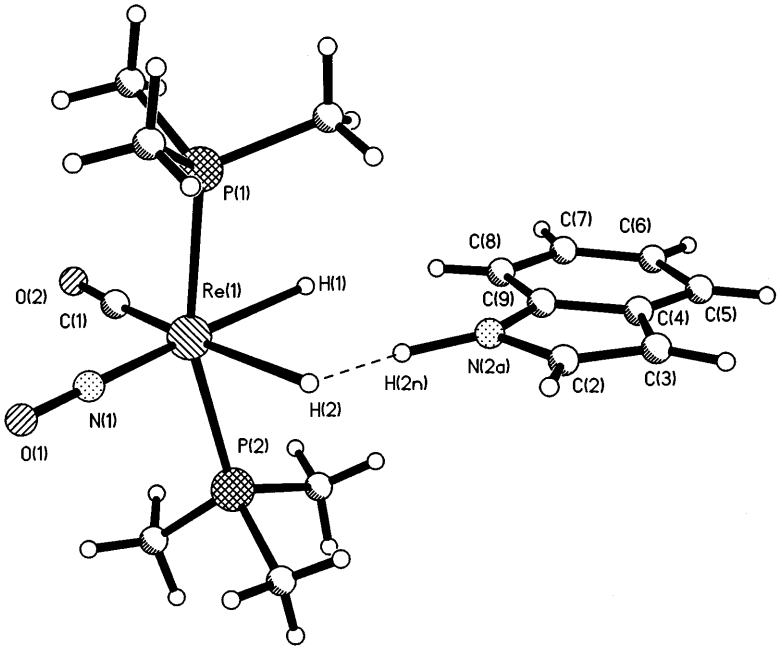

Fig. 6. Molecular structure of **2a**–indole.

bonyl Re(I) hydrides by X-ray method [16a] and by neutron diffraction for complexes ReH_5L_3 (L = $PMePh_2$ [16b], PPh_3 [1b]). The second 'long' Re–H(2) bond is positioned in front of an elongated NH fragment of indole (N–H, 1.28(3) Å). In this case the H(2)···H(2n)–N(2a) contact (1.79(5) Å) is very similar to the interaction in $ReH_5(PPh_3)_3$·indole [1b] (H···H, 1.734 Å). The additional interaction between hydride H(1) and NH indole fragment is very weak and the H···H(N) distance (2.21 Å) is comparable to the H···HN distance in $ReH_5(PPh_3)_3$·indole [1b] and is close to the sum of van der Waals radii for H···H = 2.4 Å. An explanation for this might be that crystal packing could enforce the second binding mode or/and that the weak interaction might be accompanied by a loss of selectivity [3].

2.4. Hydrogen bonds $MH^{\delta-}\cdots^{\delta+}HX$ and a proton transfer to rhenium hydrides

2.4.1. Complexes **2:1**

Low temperature interaction of the $ReH_2(CO)(NO)(PR_3)_2$ hydrides with trifluoroacetic acid is known [17] to result in the formation of dihydrogen complexes which are kinetic products of protonation of these hydrides. In order to generate the situation close to that with possible proton transfer we increased substantially the concentration of the strongest alcohol PFTB.

Table 3
Summary of crystallographic data, details of intensity collection, and least squares refinement parameters of the complex **2a**–indole and **5a**

Compound	**2a**–indole	**5a**
Formula	$C_{15}H_{27}N_2O_2P_2Re$	$C_{13}H_{23}N_2O_5P_2Re$
*F*w	515.5	535.5
Color and habit	Yellow, prism	Orange, prism
Space group	$P2_1/c$	$P2_1/c$
a (Å)	13.161(3)	12.853(9)
b (Å)	11.916(2)	12.260(8)
c (Å)	13.411(3)	12.774(9)
β (°)	98.62(2)	91.71(2)
V (Å^3)	2079.5(8)	2012(2)
Z	4	4
D_{calc} (g cm^{-3})	1.647	1.768
μ (mm^{-1})	6.004	6.220
Scan type	θ–2θ	θ–2θ
Scan speed	Variable, 2.02–14.65	Variable, 2.02–14.65
Scan width (°)	2.00	2.00
2θ Range (°)	2–50	2–48
Unique data	3331	6066
Reflections observed	2321 ($F>4\sigma$)	2338 ($F>4\sigma$)
Weighting scheme	$w^{-1}=\sigma^2(F)+0.0042F^2$	$w^{-1}=\sigma^2(F)+0.0026F^2$
R [a]	0.048	0.054
R_w [b]	0.063	0.067
Residual extrema in final difference map (e Å^{-3})	2.14–1.54	1.82–1.78

[a] $R=\Sigma(|F_o|-|F_c|)/\Sigma|F_o|$.
[b] $R_w=\Sigma w^{1/2}(|F_o|-|F_c|)/\Sigma w^{1/2}|F_o|$.

Table 4
Main geometric parameters for compound **2a**–indole

Bond lengths (Å)			
Re(1)–P(1)	2.393(3)	Re(1)–P(2)	2.399(3)
Re(1)–N(1)	1.866(9)	Re(1)–C(1)	1.854(9)
Re(1)–H(1)	1.626(28)	N(1)–O(1)	1.179(14)
O(2)–C(1)	1.171(13)	N(2a)–H(2n)	1.277(27)
N(2a)–C(2)	1.411(1)	N(2a)–C(9)	1.389(13)
C(2)–C(3)	1.341(14)	C(3)–C(4)	1.435(16)
C(4)–C(9)	1.378(15)		
Bond angles (°)			
P(1)–Re(1)–P(2)	161.9(1)	P(1)–Re(1)–N(1)	96.3(3)
P(2)–Re(1)–N(1)	96.6(3)	P(1)–Re(1)–C(1)	95.4(3)
P(2)–Re(1)–C(1)	94.3(3)	N(1)–Re(1)–C(1)	102.1(4)
Re(1)–N(1)–O(1)	179.4(9)	Re(1)–C(1)–O(2)	177.7(9)
C(2)–N(2a)–C(9)	105.2(5)	N(2a)–C(2)–C(3)	110.4(6)
C(2)–C(3)–C(4)	108.0(10)	N(2a)–C(9)–C(8)	125.3(9)
C(3)–C(4)–C(9)	105.8(10)	N(2a)–C(9)–C(4)	110.7(9)

However the proton transfer has never been observed. Instead the coordination of the second alcohol molecule takes place. And despite the diversity of monocoordinated complexes **2** upon this coordination the hydride atom appears to be hydrogen bonded in each doublecoordinated complex **3**. However it is not possible to distinguish which of two hydride atoms takes part in the hydrogen bond formation [3]. The new high-frequency ν_{CO} band ($\Delta\nu = +25$ cm^{-1}) appears with the position for 12–13 cm^{-1} higher than ν_{CO} for the 1:1

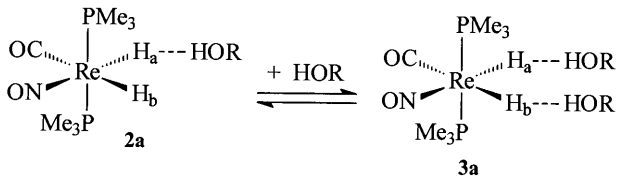

Scheme 2.

hydrogen bonded complexes **2** or **2′**. There is also new ν_{NO} band shifted to higher frequency range compare to the ν_{NO} band of the 1:1 hydrogen bonded complexes **2** or **2′** (Table 5). The intensity of these bands increases on decreasing the temperature and the bands ν_{CO} and ν_{NO} of the 1:1 complex decrease in intensity with an isobestic point.

It is interesting that in the case of **1b** only the adduct **2′b** with NO···HOR bond gives the 2:1 complex (**3′b**) (Scheme 1). The high frequency band at 1661 cm^{-1} belonging to the ν_{NO} vibrations of the 1:1 complex **2b** of H···H type remains unchanged upon cooling and increase of PFTB concentration, whereas the ν_{NO} band at 1592 cm^{-1} under these conditions decreases and new high-frequency band at 1613 cm^{-1} appears (Fig. 7). The intensity growth of the low frequency shoulder on the ν_{ReH} band corresponds to the increase of the bonded hydride groups content. The hydride atom in the complex **3′b** takes part in the hydrogen bonding together with nitrosyl group (Scheme 1).

Table 5
IR data in the range of ν_{CO} and ν_{NO} vibrations (cm^{-1}) for the hydrides **1** and their hydrogen bonded complexes **2** and **3** (of 1:1 and 2:1 composition, respectively) in hexane at 200 K

	ν_{CO} (**1**)	ν_{CO} (**2**)	ν_{CO} (**3**)	ν_{NO} (**1**)	ν_{NO} (**2**)/$\Delta\nu_{NO}$ [a]	ν_{NO} (**3**)/$\Delta\nu_{NO}$ [b]
1a	1962	1973	1986	1652	1671/+19, 1597/−55	1686/+15, 1622/+25
1b	1957	1968	1980	1650	1666/+16, 1592/−58	1613/+21
1c	1952	1963	1975	1645	1592/−53	1625/+33
1d	1966	1977	1987	1673	1689/+16	1710/+21

[a] $\Delta\nu_{NO} = \nu_{NO}$ (**2**) − ν_{NO} (**1**).
[b] $\Delta\nu_{NO} = \nu_{NO}$ (**3**) − ν_{NO} (**2**).

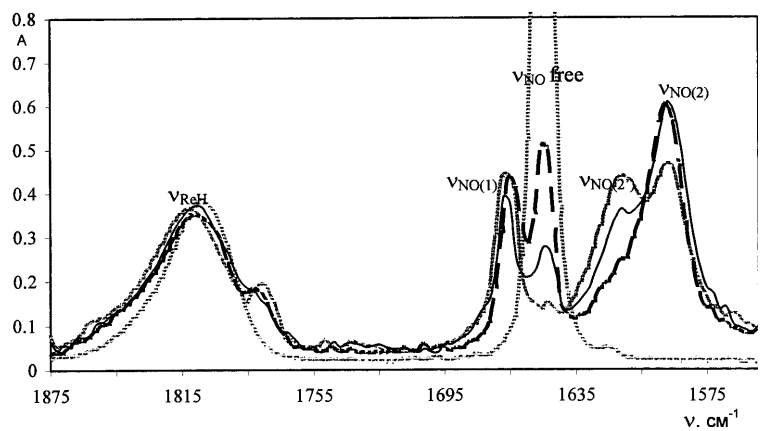

Fig. 7. IR spectra in the ν_{ReH} and ν_{NO} range of the hydride **1b** (0.008 mol l^{-1}) in the presence of PFTB (0.080 mol l^{-1}) in hexane.

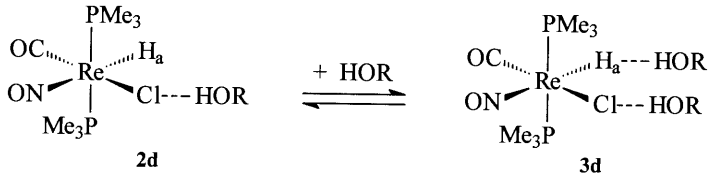

Scheme 3.

Only in the spectrum of **1a** new band ν_{NO} lies higher than that of both the initial hydride **1a** and the 1:1 complex **2a** with H···H bond (1686 cm^{-1}) similarly to ν_{CO} bands. The intensity of this band belonging to the adduct **3a** with two H···H bonds increases on cooling (Scheme 2).

In the case of **1d**, the 2:1 complex formation also leads to appearance of new high-frequency ν_{NO} band (1710 cm^{-1}), which is attributed to the doubly hydrogen bonded complex **3d** with ReCl···HOR and ReH···HOR bonds (Scheme 3).

All processes in Schemes 1–3 are reversible and the increase of temperature causes the shift to the 1:1 complexes. Thus hydrogen-bonded complexes under conditions approaching proton transfer certainly have hydride atom as the site of coordination.

The (η^2-H_2) cationic complex **4a** was not detected in the reaction of **1a** with fluorinated alcohols and phenols but the final product of the interaction between **1a** and *p*-nitrophenol–$ReH(p\text{-}OC_6H_4NO_2)(CO)(NO)(PMe_3)_2$ (**5a**) was isolated, characterized by IR spectroscopy, and studied by single crystal X-ray analysis. The IR spectrum of the product **5a** shows the bands ν_{CO} (1996 cm^{-1}), ν_{ReH} (1808 cm^{-1}), ν_{NO} (1665 cm^{-1}). They are slightly higher than those in the hydrogen bonded complex **2a**–*p*-nitrophenol (Table 2). Notably, the bands $\nu^{as}_{NO_2}$ (1489 cm^{-1}), $\nu^{s}_{NO_2}$ (1299 cm^{-1}), ν_{Ar} (1581 cm^{-1}) characteristic for *p*-nitrophenolate are observed. They are shifted to lower frequencies in comparison to the corresponding bands in free *p*-nitrophenol and the hydrogen bonded complex **2a**–*p*-nitrophenol. The X-ray data for orange crystals of complex **5a** (Tables 3 and 6) show that *p*-nitrophenolate ligand is in the *trans*-position to the CO-group (Re–O 2.11(1) Å, C–Re–O 167.6°, Re–C, 1.89(2); C–O, 1.17(2) Å) (Fig. 8). The *trans*-fragment PReP (Re–P, 2.433(4); 2.422(4) Å, P–Re–P 166.5°) is orthogonal to the plane of Re(1), oxygen atom of *p*-nitrophenolate fragment, CO and NO ligands (Re–N, 1.79(1); N–O, 1.18(2) Å) and hydride atom (Re–H, 1.90(6) Å) the position of which was determined from the differences range and not refined. It is noteworthy that similar geometry was found [17] for $ReH(\eta^1\text{-}OCOCF_3)(PMe_3)_2(NO)(CO)$ obtained as a product of protonation of **1a** by trifluoroacetic acid (TFA). This allows us to assume that interaction of the rhenium hydride **1a** with *p*-nitrophenol and TFA goes along the same reaction pathway leading to the same product — the organyloxy-derivative.

In order to observe the proton transfer with the formation of dihydrogen complex we studied the interaction of **1a** with stronger proton donor such as TFA. We used the conditions which allowed to observe (η^2-H_2)-complex by NMR [17], namely the 1:1 and 1:4 ratio of **1a**–CF_3COOH at 200 K in dichloromethane. The IR spectra under these conditions revealed new bands ν_{CO} (2053 cm^{-1}), ν_{ReH} (1863 cm^{-1}) assigned to the vibrations of the dihydrogen complex $[ReH(\eta^2\text{-}H_2)(CO)(NO)(PMe_3)_2]^+$ (**4a**) (Table 7). This assignment was made on the base of variable temperature experiments at different TFA concentrations and is in agreement with significant high frequency shifts of ν_{CO}, ν_{MH}, and ν_{NO} upon the protonation ($\Delta\nu = 60$–100 cm^{-1}) [6]. The bands corresponding to the monotrifluoroacetate $ReH(\eta^1\text{-}OCOCF_3)(CO)(NO)(PMe_3)_2$ (**5a**–**TFA**) ν_{CO} (1974 cm^{-1}), ν_{ReH} (1822 cm^{-1}), ν^{as}_{OCO} (1704 cm^{-1}) appear and intensify in time at the temperature above 220 K. The assignment of ν_{NO} bands in both **4a** and **5a**–TFA is rather ambiguous because of presence of the ν^{as}_{OCO} bands of TFA in the same spectral region. However we assume that the bands 1743 and 1668 cm^{-1} could be attributed to the complexes **4a** and **5a**–TFA correspondingly. The content of the (η^2-H_2)-complex slightly increases from equimolar to 4-fold

Table 6
Main geometric parameters for compound **5a**

Bond lengths (Å)			
Re(1)–P(1)	2.433 (4)	Re(1)–P(2)	2.422 (4)
Re(1)–O(3)	2.106 (10)	Re(1)–N(1)	1.796 (11)
Re(1)–C(1)	1.882 (15)	Re(1)–H(1)	1.90(6)
O(1)–C(1)	1.166 (19)	O(2)–N(1)	1.182 (16)
O(3)–C(8)	1.313 (15)	O(4)–N(2)	1.224 (17)
O(5)–N(2)	1.232 (18)	N(2)–C(11)	1.445 (17)
C(8)–C(9)	1.401 (18)	C(8)–C(13)	1.410 (17)
C(9)–C(10)	1.382 (18)	C(10)–C(11)	1.366 (17)
C(11)–C(12)	1.386 (18)	C(12)–C(13)	1.399 (17)
Bond angles (°)			
P(1)–Re(1)–P(2)	166.5(1)	P(1)–Re(1)–O(3)	84.1(3)
P(2)–Re(1)–O(3)	87.9(3)	P(1)–Re(1)–N(1)	96.7(4)
P(2)–Re(1)–N(1)	95.2(4)	O(3)–Re(1)–N(1)	98.4(4)
P(1)–Re(1)–C(1)	92.7(4)	P(2)–Re(1)–C(1)	92.8(4)
O(3)–Re(1)–C(1)	167.7(5)	N(1)–Re(1)–C(1)	93.8(6)
Re(1)–O(3)–C(8)	137.7(8)	Re(1)–N(1)–O(2)	167.7(10)
O(4)–N(2)–O(5)	124.2(12)	O(4)–N(2)–C(11)	118.6(12)
O(5)–N(2)–C(11)	117.2(11)	Re(1)–C(1)–O(1)	176.9(13)
O(3)–C(8)–C(9)	120.0(11)	O(3)–C(8)–C(13)	120.4(11)
N(2)–C(11)–C(10)	119.7(11)	N(2)–C(11)–C(12)	119.2(12)

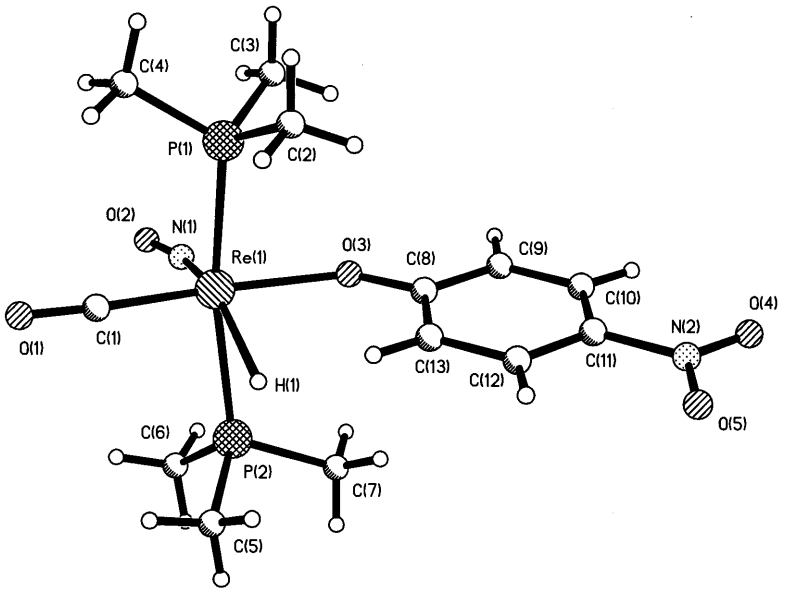

Fig. 8. Molecular structure of **5a**.

excess of TFA and the monotrifluoroactate appears already at 200 K. These results are in accordance with the data of NMR studies [17] showing that at 200 K in CD_2Cl_2 the (η^2-H_2)-complex, the initial hydride and the monotrifluoroacetate coexist. Both time and temperature increase result in the formation of not only mono- but also di-acetates (Table 7).

However, bands of free hydride **1** and dihydrogen bonded one (**2**) are not separated in the CH_2Cl_2 solution. Moreover the hydrogen bond formation constants in this solvent are less than in nonpolar one. Therefore we studied the interaction between **1a** and TFA in hexane. At the equimolar ratio of the acid and hydride at 200 K the acetate formation is suppressed and co-existence of initial hydride **1a**, ReH···HO complex **2a** and dihydrogen complex **4a** (Scheme 4, Fig. 9) is indicated by the presence of the corresponding ν_{CO} and ν_{NO} bands in the IR spectra (Table 7). The ν_{ReH} bands of **1a** and **2a** are overlapped with the ν_{CO} bands of trifluoroacetic acid. The ν_{CO} band at 2050 cm^{-1} of the cationic dihydrogen complex **4a** is shifted to the high-frequency range as in the CH_2Cl_2 solution. The bands at 1860 and 1745 cm^{-1} are assigned to the ν_{ReH} and ν_{NO} vibrations of the complex **4a** (Fig. 9). So, under conditions where further transformation of dihydrogen complex is suppressed, the equilibrium between the **1a**, **2a** and **4a** complexes is observed. The bands of the dihydrogen bonded complex **2a** and the non-classical complex **4a** disappear with increase of temperature or the acid concentration while the bands related to the corresponding acetate appear and grow up.

Changes in the IR spectra of the monohydride **1d** in the presence of equimolar amount or slight excess of TFA are similar to those of the dihydride **1a** confirming similar protonation mechanism. Herein again new higher frequency bands ν_{CO} (2010 cm^{-1}) and ν_{NO} (1758 cm^{-1}) belonging to the (η^2-H_2)-complex **4d** arise at 200 K in the presence of the acid. Even small temperature increase (up to 220 K) leads to hydrogen evolution and formation of the monoacetate **5d**.

So, we suggest that the mechanism of protonation of transition metal hydrides leading through dihydrogen bonding to (η^2-H_2) complexes (Scheme 6) has general character [18]. In our opinion the evidence of such proton transfer pathways should be obtained from combined IR and NMR studies allowing to overcome weak points of each method. The difficulties in distinguishing H···H complex and initial hydride by NMR are well known. Usually, hydride signal in the NMR spectra is an average of the fast exchanging signals of monomer and hydrogen bonded complex [2,3,18]. Recently the increase of H–H coupling constant J_{ab} (resulting from quantum exchange) upon hydrogen bonding was found [19]. Only once at 96 K in liquid freons, two different signals separated by 1.2 ppm were observed [2c]. The IR spectroscopy has the advantage

Table 7
IR spectra of the hydride interaction products of the $ReH_2(CO)(NO)(PMe_3)_2$ (**1a**) and CF_3COOH in CH_2Cl_2

	ν_{CO}	ν_{ReH}	ν_{NO}	ν^{as}_{OCO}
(η^2–H_2)–complex	2050 [a]	1860 [a]	1745 [a]	
4a	2053	1863	1743	
Mono(η^1-$OCOCF_3$)	1975	1820	1668	1704
Di(η^1-$OCOCF_3$)	2009		1708	1762

[a] Data in hexane.

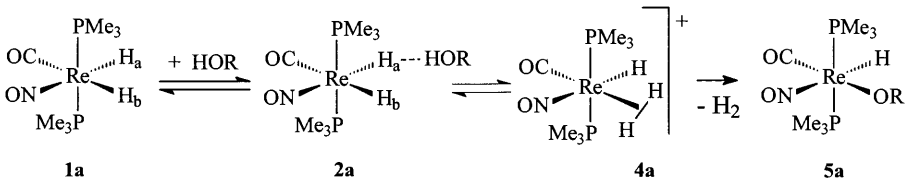

Scheme 4.

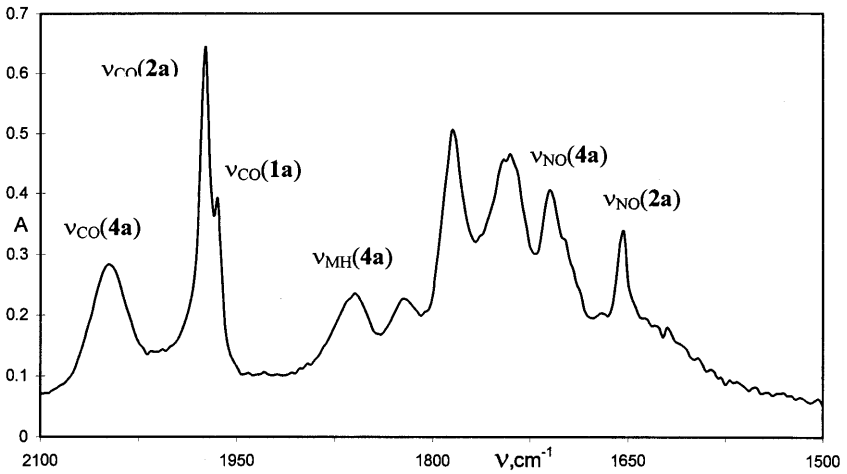

Fig. 9. IR spectra of hydride **1a** in the presence of CF_3COOH in hexane at 200 K.

not only giving the evidence of hydrogen bond formation (from ν_{XH} band changes) but also allowing to detect separated bands of initial hydride, hydrogen bonded and dihydrogen complexes at the same time.

3. Conclusion

Varying the concentration and strength of proton donor (from indole to phenol, HFIP, PFTB, and trifluoroacetic acid) we elucidated all steps of protonation of the rhenium hydrides $ReHX(CO)(NO)(PR_3)_2$ (**1**). The formation of medium strength hydrogen bonds of different types is determined by the proton accepting properties of different ligands. Steric hindrances of phosphine ligands can induce the change of coordination site in **1a**–**c**, then the electronic effect of chlorine in **1d** disables the proton accepting ability of hydride ligand in this complex. However, it is the hydrogen bonding to hydride atom as proton acceptor that precedes the proton transfer followed by the formation of cationic dihydrogen complex. Proton transfer from the hydrogen bonded complex ReH···HO to the dihydrogen complex is observed in low polar and nonpolar media at low temperatures. Unfortunately further transformations of the latter to the mono- and diacetates prevent to determine quantitative characteristics of the equilibrium between ReH···$HOCOCF_3$ and the $[Re(\eta^2\text{-}H_2)]^+$ complex. The use of more stable dihydrogen complexes or lowering temperature could allow to obtain this kind of data (the problem is under our active investigation). We believe that the formation of hydrogen bond with hydride atom as proton acceptor at the first step of protonation leading to dihydrogen complex formation has a general character for transition metal hydrides.

4. Experimental

The dihydrides $ReH_2(CO)(NO)L_2$ studied in this work were prepared as described [17].

4.1. Preparation of *2a*–indole monocrystals

To solution of 0.05 g (0.12 mM) of $ReH_2(CO)(NO)(PMe_3)_2$ (**1a**) in 3 ml of hexane the indole solution (0.015 g, 0.13 mM) in hexane was added. The mixture was refrigerated at -5°C for 24 h. The yellow prismatic crystals formed were separated, washed with cold pentane and dried at r.t. in the stream of argon.

4.2. Preparation of *5a*

To solution of 0.1 g (0.25 mM) of $ReH_2(CO)(NO)(PMe_3)_2$ (**1a**) in 10 ml of hexane solution of 0.042 g (0.30 mM) of *p*-nitrophenol in 5 ml of dichloromethane was added. The mixture was heated under reflux for 1 h. The orange solution formed was

concentrated at 40°C and 0.1 Torr to the volume of 5 ml and refrigerated at −5°C for 48 h. The large orange crystals formed were separated, washed with cold pentane, and dried at r.t. in the stream of argon. Yield 0.12 g (90%). ^{1}H-NMR (CD_2Cl_2): δ 2.55 (t, 1H, Re–H), 1.7 (t, 18H, CH_3), 6.95 (d, 2H), 8.1 (d, 2H). Anal. Calc. for $C_{13}H_{23}N_2O_5P_2Re$: C, 29.10; H, 4.51; N, 5.22. Found: C, 28.98; H, 4.45; N, 5.16%.

IR measurements were performed on a 'Specord M80' and 'Specord M82' spectrometer. Spectra were recorded for Nujol mulls and for the films in the range 4000–400 cm^{-1} and in solutions in concentration 10^{-1}–10^{-4} mol l^{-1} in CaF_2 and CsI cells 0.01–2 cm. All manipulations were performed in an atmosphere of dry argon. Freshly distilled anhydrous oxygen-free solvents were distilled. The study of hydrogen bonds in the range of stretching vibrations of XH-groups of proton donors were carried out at concentrations excluding self-association of acid ($C = 1 \times 10^{-3}$–1×10^{-2} mol l^{-1}) in the presence hydride excess ($C = 2 \times 10^{-2}$–7×10^{-1} mol l^{-1}). Studies in the range of stretching vibrations of ligands of the rhenium hydride complexes were carried out in the presence of equimolar amounts or of excess of proton donors.

Low temperature measurements were carried out in cryostat (Carl Zeiss Jena) in the temperature range 190–290 K using a stream of liquid nitrogen. The accuracy of temperature adjustment was ±0.5 K. Cells width was 0.04–0.12 cm. In the cases of proton transfer studies the reagents were mixed at low temperatures. Then the cold solutions were transferred into the cryostat precooled to necessary temperature.

Positions of ν_{XH} (bonded) bands correspond to their center of gravity ($s = 3$ cm^{-1}). Enthalpy values ($-\Delta H$, kcal mol^{-1}) were determined both from spectral data ($\Delta\nu_{XH}$ and integral intensities A) using correlation equations **1**, **2** and from temperature dependence of formation constants (ln K vs. $1/T$). The $-\Delta H$ accuracy in the first case was ±0.4 kcal mol^{-1}. Formation constants for every temperature were determined by the decrease of ν_{CO} and ν_{NO} optical density of bands of free carbonyl and nitrosyl groups.

4.3. Crystal structure determinations

The crystals were all mounted in air on glass fibers using 5 min epoxy resin. The unit cells were determined and refined from 24 equivalent reflections with $2\theta >$ 22–28° and obtained from Siemens R3PC four-circle diffractometer at r.t. for **5a** and at temperature 161 K for **2a**–indole.

Three reflections were monitored periodically for each compound as a check for crystal decomposition or movement. No significant variation in these standards was observed, so no correction was applied. Details of crystal parameters, data collection and structure refinement are given in Table 3.

All structures were solved by direct methods to locate the rhenium and phosphorus atoms. For adduct **2a**–indole at this stage, all non-hydrogen atoms were found. The other atoms in **5a** were located in the subsequent difference Fourier maps. The DIFABS method [20] was used for the absorption correction at the stage of the isotropic approximation. An anisotropic refinement was applied to all non–hydrogen atoms, and all hydrogen atoms in the structures were found from difference Fourier maps. The positions of the atoms H(1), H(2) and H(2n) of **2a**–indole were refined in the isotropic approximation. The positions of the other hydrogen atoms were refined as fixed contributions with the constant isotropic temperature factor $u_{iso} = 0.08$ Å^2. The computations were performed using the SHELXTL PLUS program package [21]. Selected bond lengths and angles for complexes studied are given in Tables 4 and 6.

5. Supplementary data

Complete lists of the bond lengths and angles and the tables of thermal parameters have been deposited at the Cambridge Crystallographic Data Center, CCDC Nos. 141849 and 141850 for **2a**–indole and **5a**, respectively. Copies of this information may be obtained free of charge from The Director, 12 Union Road, Cambridge CB2 1EZ, UK (fax: +44-1223-336033; e-mail: deposit@ccdc.cam.ac.uk or www: http://www.ccdc.cam.ac.uk).

Acknowledgements

The authors thank the Russian Foundation for Basic Research for financial support (grant No 99-03-33270) and Professor H. Berke (Zürich) and his colleagues for fruitful collaboration.

References

[1] (a) J. Wessel, B.P. Patel, R.H. Crabtree, J. Chem Soc. Chem. Commun. (1995) 2175. (b) J. Wessel; J.C. Lee Jr., E. Peris, G.P.A. Yap, J.B. Fortin, J.S. Ricci; G. Sini, A. Albinati, T.F. Koetzle, O. Eisenstein, A.L. Rheingold, R.H. Crabtree, Angew. Chem. Int. Ed. Eng. 34 (1995) 2507. (c) B.P. Patel, J. Wessel, W. Yao, J.C. Lee Jr., E. Peris, T.F. Koetzle, G.P.A. Yap, J.B. Fortin, J.S. Ricci, G. Sini, A. Albinati, O. Eisenstein, A.L. Rheingold, R.H. Crabtree, New J. Chem. 21 (1997) 413. (d) P. Desmurs, K. Kavallieratos, W. Yao, R.H. Crabtree, New J. Chem. 23 (1999) 1111. (e) E. Peris, J.C. Lee Jr., J.R. Rambo, O. Eisenstein, R.H. Crabtree, J. Am. Chem. Soc. 117 (1995) 3485.

[2] (a) E.S. Shubina, N.V. Belkova, A.N. Krylov; E.V. Vorontsov, L.M. Epstein, D.G. Gusev, M. Niedermann, H. Berke, J. Am. Chem. Soc. 118 (1996) 1105. (b) N.V. Belkova, E.S. Shubina,

A.V. Ionidis, L.M. Epstein, H. Jacobsen, M. Niedermann, H. Berke, Inorg. Chem. 36 (1997) 1522. (c) E.S. Shubina, N.V. Belkova, A.V. Ionidis, N.S. Golubev, S.N. Smirnov, L.M. Epstein, Izv. Akad. Nauk Ser. Khim. 7 (1997) 1405; Russ. Chem. Bull. 44 (1997) 1349. (d) L.M. Epstein, E.S. Shubina, Ber. Bunsenges. Phys. Chem. 102 (1998) 359 (e) E.S. Shubina, N.V. Belkova, L.M. Epstein, J. Organomet. Chem. 536–537 (1997) 17.

[3] A. Messmer, H. Jacobsen, H. Berke, Chem. Eur. J. 5 (1999) 3341.

[4] A.V. Iogansen, The Hydrogen Bond, Nauka, Moscow, 1981, p. 134.

[5] (a) B.V. Lokshin, S.G. Kazarian, A.G. Ginzburg, Izv. Akad. Nauk SSSR Ser. Khim. (1988) 333. (b) P.A. Hamley, S.G. Kazarian, M. Poliakoff, Organometallics, 13 (1994) 1767.

[6] (a) R.B. Girling, P. Grebenic, R.N. Perutz, Inorg. Chem 25 (1986) 31. (b) B. Ma, C.L. Collins, H.F. Schaefer, J. Am. Chem. Soc. 118 (1996) 870.

[7] S.G. Kazarian, P.A. Hamley, M. Poliakoff, J. Am. Chem. Soc. 115 (1993) 9069.

[8] D.V. Yandulov, K.G. Caulton, N.V. Belkova, E.S. Shubina, L.M. Epstein, D.V. Khoroshun, D.G. Musaev, K. Morokuma, J. Am. Chem. Soc. 120 (1998) 12553.

[9] (a) A.V. Iogansen, Theor. Experim. Khim. 7 (1971) 314. (b) A.V. Iogansen, Theor. Experim. Khim. 7 (1971) 302. (c) A.V. Iogansen, Spectrochim. Acta 35A (1999) 1585.

[10] Equilibrium concentrations were determined from the decrease of the intensity of bands $\nu_{\mathrm{CO\ free}}$ and $\nu_{\mathrm{NO\ free}}$ in the presence of PFTB for every temperature value.

[11] The empirical Iogansen 'rule of factors' [9] demonstrating the invariability of proton donor (P_i) and proton acceptor (E_j) properties of organic acids and bases in hydrogen bonding was obtained from a large array of spectral and colorimetric data. We used the following equation of 'rule of factors' $(-\Delta H_{ij}) = (-\Delta H_{11})P_iE_j$ where $(-\Delta H_{11})$ – enthalpy of hydrogen bonding for a standard pair: phenol–diethyl ether ($P_{11} = E_{11} = 1.00$). The $-\Delta H_{11}$ value is solvent dependent and for carbon tetrachloride is equal to 5.3 kcal mol^{-1}, for hexane, 5.7 kcal mol^{-1} [9b]. Thus the values E_j do not depend on proton donor and media.

[12] (a) D. Nietlispach, V.I. Bakhmutov, H. Berke J. Am. Chem. Soc.115 (1993) 9193. (b) R.G. Pearson, Chem. Rev. 85 (1985) 41.

[13] C. Tolman, Chem. Rev. 77 (1977) 313.

[14] G. Orlova, S. Sheiner, J. Phys. Chem. A 102 (1998) 4813.

[15] (a) D. Veghini, H. Berke, Inorg. Chem. 35 (1996) 4770. (b) D. Veghini, S.E. Nefedov, H. Schmalle, H. Berke, J. Organomet. Chem. 526 (1996) 117.

[16] (a) D.G. Gusev, D. Nietlispach, I.L. Eremenko, H. Berke, Inorg. Chem. 32 (1993) 3628. (b)T.J. Emge, T.F. Koetzle, J.W. Bruno, K.G. Caulton, Inorg. Chem. 23 (1984) 4012.

[17] S. Feracin, T. Burgi, V.I. Bakhmutov, I. Eremenko, E.V. Vorontsov, A.V. Vymenits, H. Berke, Organometallics 13 (1994) 4194.

[18] (a) E.S. Shubina, N.V. Belkova, E.V. Bakhmutova, E.V. Vorontsov, V.I. Bakhmutov, A.V. Ionidis, C. Bianchini, L. Marvelli, M. Peruzini, L.M. Epstein, Inorg. Chim. Acta 280 (1998) 302. (b) J.A. Ayllon, C. Gervaux, S. Sabo-Etienne, B. Chaudret, Organometallics 16 (1997) 2000.

[19] S. Gruendemann, S. Ulrich, H.H. Limbach, N.S. Golubev, G.S. Denisov, L.M. Epstein, S. Sabo-Etienne, B. Chaudret, Inorg. Chem. 38 (1999) 2550.

[20] N. Walker, D. Stuart, Acta Crystallogr. Sect. A 39 (1983) 158.

[21] G.M. Sheldrick, Crystallographic computing, in: Data Collection, Structure Determination, Proteins and Databases, vol. 3, 1985, p. 175.